Engineering Failure Analysis 150 (2023) 107325

Contents lists available at ScienceDirect

Engineering Failure Analysis

journal homepage: www.elsevier.com/locate/engfailanal

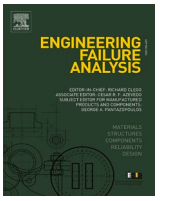

Cracking failure analysis due to fatigue of the Ti-6Al-4V alloy coated with SiC layer and Cr interlayer deposited by magnetron sputtering

Alexandra A. Arbex [a], Luis Reis [b], Gisele F.C. Almeida [a,*], Abrão C. Merij [a], Marcos Massi [a], Antônio A. Couto [a,c]

[a] Engineering School, Mackenzie Presbyterian University, Rua da Consolação, 930 - Consolação, São Paulo, SP 01302-907, Brazil
[b] IDMEC, Instituto Superior Técnico, Universidade de Lisboa, Av. Rovisco Pais 1, 1049-001 Lisbon, Portugal
[c] CECTM, Materials Science and Technology Center, Nuclear and Energy Research Institute, Ave. Lineu Prestes, 2242 - Cidade Universitária, São Paulo, SP CEP 05508-000, Brazil

ARTICLE INFO

Keywords:
Fatigue
Ti-6Al-4V
Thin films
HIPIMS
Fractography

ABSTRACT

This work aimed to study the effects of coating a thin film of Silicon Carbide and chromium interlayer on the fatigue behavior of Ti-6Al-4V alloy and the correspondent failure evaluation. In the characterization of the layer, the roughness, thickness, and adhesion were determined. Uniaxial fatigue tests were performed under R = 0.1 and the fracture surfaces and corresponding failure mechanisms were observed and identified by SEM, respectively. In the specimens coated using the DC source the number of cycles to failure of the fatigue was increased. The fracture surfaces showed that the crack initiation occurred in the internal regions of the specimens and not superficially. In this case, the layer remained adhered to the specimens even after the tests, showing the effectiveness of the film. In specimens coated using the HiPIMS source, the number of cycles to failure decreased, the cracks were mostly superficial, and the deposited film showed low adhesion after the tests. It proved to be ineffective, worsening the material fatigue behavior.

1. Introduction

Titanium and its alloys have applications in the aeronautical, aerospace, chemical, and petrochemical industries [1], sports materials [2], among others. Hip Prostheses with ever-increasing life, even if under fatigue loading are made of Ti-6Al-4V [3]. This alloy is the most used titanium alloy, having great properties such as high mechanical strength/weight ratio, excellent fatigue, and corrosion resistance [4]. The development of products in different industries is related to advances in surface engineering techniques. The use of modern coating materials and methods of coating deposition has allowed manufacturers to produce elements and structures that withstand aggressive environments and harsh working conditions [5]. The Ti-6Al-4V alloy in more severe applications led to several studies being carried out to improve its properties, such as fatigue and wear resistance [6].

Structural failure is often caused by fatigue cracks which frequently initiate and propagate in the critical regions as the free surface, with microcracks that later propagate to inner regions [7]. Thus, strengthening component's surfaces is an important strategy to delay the onset of fatigue cracking [8]. They can be improved for instance introducing compressive residual stresses, among other techniques

* Corresponding author.
E-mail address: gisele.almeida@mackenzie.br (G.F.C. Almeida).

https://doi.org/10.1016/j.engfailanal.2023.107325
Received 16 March 2023; Received in revised form 21 April 2023; Accepted 7 May 2023
Available online 11 May 2023

that are being studied [4].

The useful life of materials can be improved by applying thin films of hard ceramics such as nitride and carbide films at the surfaces [9]. The hard thin film coating technique is one of the effective methods to protect the material from wear and corrosion. Some films as TiN, TiAlN, AlCrN, CrN and DLC, have been extensively studied to improve the wear and corrosion resistance of various materials that are achieved by controlling chemical composition [10] and film thickness [11]. Fatigue studies on coated parts showed different results depending on the technique used and parameters, such as the deposition temperature on the substrate [12,13], number of layers [9], layer thickness [11], film material [14], among others. Silicon Carbide (SiC) films used as a protective coating are very promising against wear of Ti-6Al-4V alloy and to improve its mechanical properties due to its excellent hardness and wear resistance [15].

Magnetron sputtering is a physical method of vapor deposition in which energetic particles bombard the surface of a target under the action of electric and magnetic fields [16]. Magnetron sputtering is applied more widely to manufacture anti-wear coating materials [17]. This method proved to be good for obtaining thin films, presenting a high deposition rate, high purity, excellent homogeneity and adhesion, and good precision in controlling film thickness and grain size. This technique can use different types of sources, such as Radio Frequency (RF), Direct Current (DC) and more recently High-Power Impulse Magnetron Sputtering (HiPIMS) has been widely used. In HIPIMS coating technique, a pulsed source of high power and short pulse width allows denser and more uniform films to be deposited [18]. Silicon Carbide (SiC) films used as a protective coating are very promising in the tribological properties of Ti-6Al-4V alloy and to improve its mechanical properties due to its high hardness and wear resistance [19].

In this work, the cracking failure analysis due to fatigue of the Ti-6Al-4V alloy coated with SiC ceramic film and Chromium interlayer was studied. The thin film was deposited by Magnetron Sputtering technique using two types of sources: DC and HiPIMS. The objective of this study is to verify the influence of these coatings on the fatigue performance of the Ti-6Al-4V alloy and on the crack nucleation micromechanisms.

2. Materials and methods

In this work, the Ti-6Al-4V alloy was used in the form of cylindrical bars with a diameter of 15 mm, in the forged condition and annealed at 800 °C for 2 h and cooled in air, having an equiaxed microstructure and all material of the bars belong to the same batch. The bar was cut into discs approximately 2 mm thick for the coating tests. The surfaces of the samples were manually polished, cleaned by ultrasound with acetone, and then the depositions were performed.

2.1. Layer deposition

SiC films were deposited on Ti-6Al-4V substrates using DC and HiPIMS sources. An interlayer of Cr was deposited to improve the adhesion between the SiC film and the substrate. All films were deposited 200 mm from the target, and an extensor was used to align the center of the fatigue specimen to the focus of the target. The working pressure and argon flow rate of 8.3×10^{-3} Pa and 100 sccm, respectively. Table 1 shows the deposition parameters. The purity of SiC and Cr targets were 99.5% and 99.95%, respectively. Using the same parameters as in Table 1, depositions were carried out on the fatigue specimens, as prepared and shown in the internal view of the plasma reactor in Fig. 1.

2.2. Layer characterization

The coated layer was characterized by X-ray diffraction to identify the compounds formed. In the analysis by X-ray diffraction, the Rigaku equipment, model Multiflex, was used, using CuKα radiation (wavelength λ of 0.1542 nm), sweeping a range of angles from 5 to 90°, with a speed of 2° per minute and step of 0.02. The Search Match software was used to identify the present phases.

The qualitative adhesion test was performed on a Rockwell C durometer, according to VDI 3198 [20], applying a load perpendicular to the sample area with a conical diamond indenter causing thin film fracture and plastic deformation of the substrate. In the test, a load of 150 kgf was applied for 30 s, causing critical shear stresses at the substrate/film interface. This impression is then evaluated under an optical microscope and its adhesion is analyzed according to Fig. 2, which illustrates the profile of films with acceptable fracture type and films with unacceptable fracture, with delamination, resulting in exposure of the substrate [21].

The scratch test was performed for adhesion analysis using the Antoon Paar Micro Combi MCT3 meter. This test consists of moving a conical diamond indenter, with a tip radius of 200 μm, applying a constant or variable load, perpendicular to the surface of the part. The defined path causes the material to be scratched until the film fails, with determination of the critical load [22].

The film thickness was measured using Atomic Force Microscopy (AFM). The AFM used was the Antoon Paar Tosca 400 model. The average roughness (Ra) was obtained both in specimens without and with HiPIMS coating.

Table 1
Chromium interlayer and SiC film deposition parameters using DC and HiPIMS sources.

	DC Source		HiPIMS Source			
	Time	Power	Time	Power	Pulse Width	Frequency
Cr	15 min	150 W	30 min	300 W	100 μs	800 Hz
SiC	45 min	150 W	90 min	300 W	100 μs	800 Hz

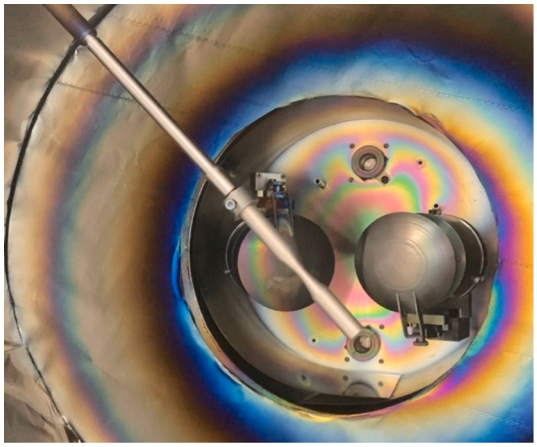

Fig. 1. Internal view of the plasma reactor in the deposition of a specimen for fatigue testing of Ti-6Al-4V alloy.

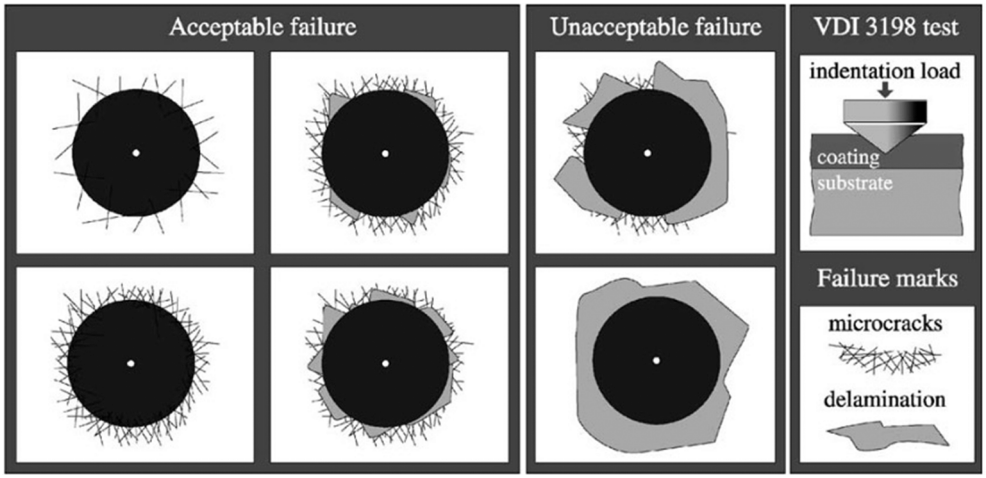

Fig. 2. The principle of VDI 3198 indentation test[20].

2.3. Tensile and fatigue tests

The tensile and fatigue specimens were machined on a CNC lathe. Tensile tests were conducted according to standard procedure ASTM E-8 M. The equipment used in the tensile tests was a servo-hydraulic Mechanical Testing machine (load capacity 250 kN) INSTRON 8502. The tensile tests were performed in order to characterize the material strength and hence define the values to carry out the fatigue tests. The ultimate tensile strength found was 955 MPa and the yield strength was 884 MPa. Uniaxial fatigue tests were performed according to ASTM E 466. The tests were performed using a sinusoidal constant amplitude load of frequency 12 Hz and stress ratio $R = 0.1$, at room temperature. The equipment used in the fatigue tests was an Instron 8502 machine, with a load capacity of 100 kN and in load control. The fatigue tests were carried out until the specimens ruptured or interrupted with 10^6 cycles. The specimens for fatigue tests were machined according to Fig. 3. From the results of the fatigue tests, the values obtained were placed in a graph stress × number of cycles to failure (S–N). Results were obtained under the following conditions: Ti-6Al-4V alloy without coating, Ti-6Al-4V alloy with SiC film coating with Chromium interlayer using DC source and Ti-6Al-4V alloy with SiC film coating

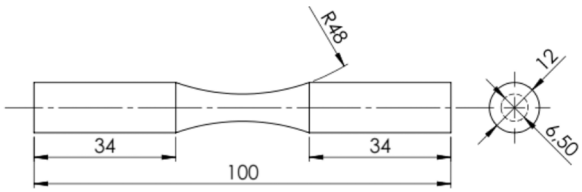

Fig. 3. Ti-6Al-4V alloy specimen used in uniaxial fatigue tests with and without SiC film coating and Cr interlayer (Dimensions in mm).

with interlayer of Chromium using HiPIMS source. After the fatigue tests, the fracture surfaces were analyzed using an optical microscope and a JEOL 200C scanning electron microscope.

3. Results and discussion

3.1. X-Ray diffraction analysis

After the deposition of the thin films with SiC and chromium interlayer using the DC source and HIPIMS in the Ti-6Al-4V samples, the present phases were analyzed by X-ray diffraction. Fig. 4 shows the X-ray diffractogram showing the phases α and β of Titanium. As the film has a nanometric thickness, it was not possible to observe and identify the film reflection, in addition to SiC being amorphous. An extra low intensity peak was observed at 44.43 degrees that it was not possible to define the present phase because it was the only one.

3.2. Layer thickness measurement

The layer thickness was measured in the Atomic Force Microscope - AFM from a silicon sample placed next to the Ti-6Al-4V alloy samples for deposition, as shown in Fig. 5. A step is left, making it possible to measure the difference in height between the film and the silicon sample, thus obtaining the thickness of the deposited layer. The AFM probe measures the step height difference, as shown in Figs. 6 and 7. Table 2 presents the thickness values of the deposited layers using the HiPIMS and DC sources. Layer thickness is an important parameter for film strength and adhesion. More homogeneous layers are less likely to have internal defects that can affect the proper functioning of the coating. Thickness depends on deposition parameters and coating material. Merij et al. [18], after carrying tests using different parameters as time and power, it was determined that the thickness of 1.67 μm had better adhesion, adding the SiC film with the Cr interlayer. At this thickness, the layer was homogeneous, after deposition by Magnetron Sputtering using the HiPIMS source [18].

In studies that performed gas nitriding [23], the films presented thicknesses of 25–65 μm, with depositions of 4 h and 10 h, with the Ion Beam Enhanced Deposited (IBED) technique [24] at 1 h of deposition, the thickness was 1.4 μm. In study with SiC coating [25], the results obtained for deposition with Magnetron Sputtering were 0.25 μm and 1 μm, with time controlled to obtain the target thicknesses. Recent studies indicate that layer thickness in ceramic films has better fatigue results with lower values, that are possible with these techniques, in the order of microns and nanometers. Another factor that can affect the fatigue result are multi-layers, rather than just one layer [11]. In the present work, the deposition parameters and source used were different, generating two different thicknesses. This difference was due to the adhesion of the layer to the substrate in each case. The layer deposited by the DC source had better adhesion at the initial thickness deposited. However, to obtain adhesion by the HiPIMS source, it was necessary to reduce the thickness of the layer deposited.

3.3. Analysis of layer adhesion

To determine if the layer was adhered to the Ti-6Al-4V alloy, a qualitative adhesion test was initially carried out with the indentation test on a Rockwell C durometer. Thus, it was possible to define whether it would be possible to initiate depositions on the fatigue specimens. The layer deposited using HiPIMS and DC sources, as per standard and visualized by optical microscopy, obtained the results shown in Fig. 8 (a and b), respectively. The images show that, according to the template in Fig. 2 of VDI 3198 standard [21], there was no film delamination during the test. Microcracks in the region close to the deformation are acceptable according to VDI 3198 [21]. It is concluded that both coatings, using HiPIMS and DC sources, have an acceptable layer adhered.

The scratch tests were carried out on the polished samples of both DC and HiPIMS depositions, with the results being a parameter to verify whether the film delaminates after a certain pull-out force, in order to use the same deposition configuration on the test specimens. The fatigue specimens have a rounded geometry in the useful area, in addition to the fact that, during deposition, the specimen rotates so that it is deposited in its entire diameter, which can affect the adhesion conditions.

Scratch testing of deposited samples was performed using an Anton Paar Micro Combi MCT3 Meter. Tables 3 and 4 show the

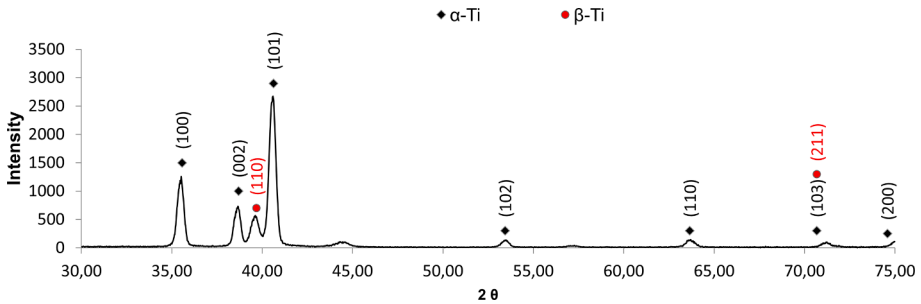

Fig. 4. X-ray diffractogram of a sample of Ti-6Al-4V alloy coated with thin film with SiC and Cr interlayer using DC source.

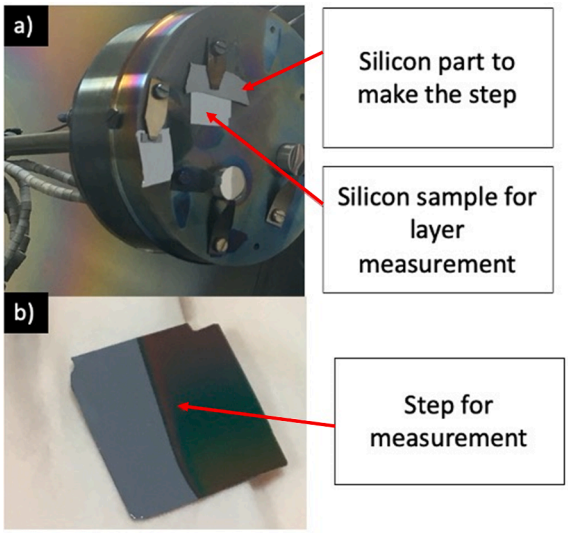

Fig. 5. Scheme used to measure the thickness of the deposited layer through the difference in the height film and the silicon sample.

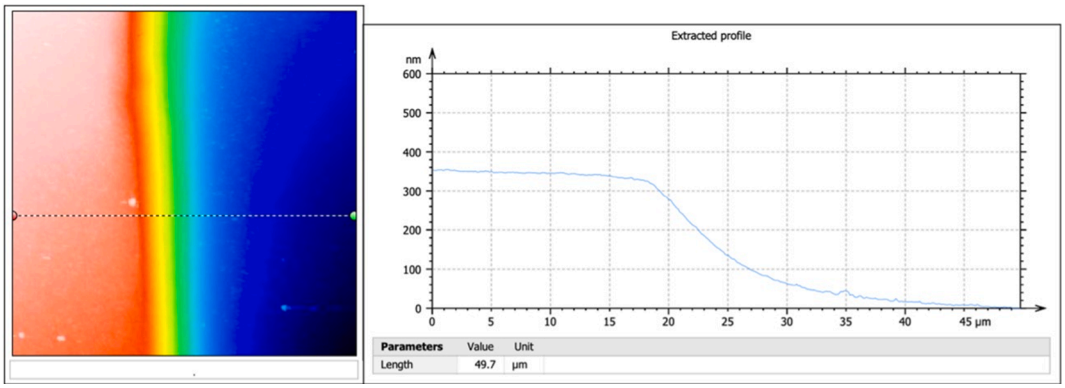

Fig. 6. The measure of the step between the silicon sample and the film in the AFM.

parameters of the scratch tests and the values of the critical loads obtained. In the sample coated using HiPIMS source, the film started to be peeled off with a load close to 1 N (LC1). However, for the substrate to be exposed, the load was approximately 35 N (LC2), which shows that the layer was well adhered. The SiC/Cr film coated using the DC source began to be peeled off with a load close to 1 N (LC1) and the substrate was exposed with a force slightly greater than 2 N (LC2).

According to Sugahara et al. [15], using the same deposition parameters with HiPIMS source, the results found for film adhesion were better, when considering the force required to delaminate the film. In this work, it is possible to observe the trail that does not present delamination up to 25 N, determined in the test. Deposition using HiPIMS source is shown in the literature as responsible for improving the adhesion of films in relation to other processes of Physical Vapor Deposition (PVD) type [26]. Bakoglidis et al. [27] investigated the effect of low temperature metal pretreatments to improve the adhesion of CNx coatings on steel substrates. The scratch tests were performed in the two most representative cases of the study: Al and W coated with a CNx film approximately 180–200 nm thick. The nanoscratch tests showed that a delamination of the CNx film occurs as a result of adhesive failure and large cracks and fragments of the film are observed at the end of the track after the test. The critical forces for this adhesion test were LC1 = 586.4 ± 102.2 µN / LC2 = 847.5 ± 31.7 µN for Al and LC1 = 917.4 ± 5 µN / 981.7 ± 18.3 µN for W.

3.4. Roughness measurements

The roughness was measured in the specimens without coating and coated with the SiC layer and Cr interlayer using the HiPIMS source. The average roughness (Ra) values obtained were similar without covering and with covering. The average values obtained were 0.32 ± 0.02 µm and 0.32 ± 0.03 µm for the uncoated and coated specimens, respectively, indicating that the roughness in the machined condition was maintained, due to the low film thickness. Roughness is an important characteristic in the fatigue properties of the material. Therefore, the finishing standard of the specimens was controlled by executing the machining on a CNC lathe with

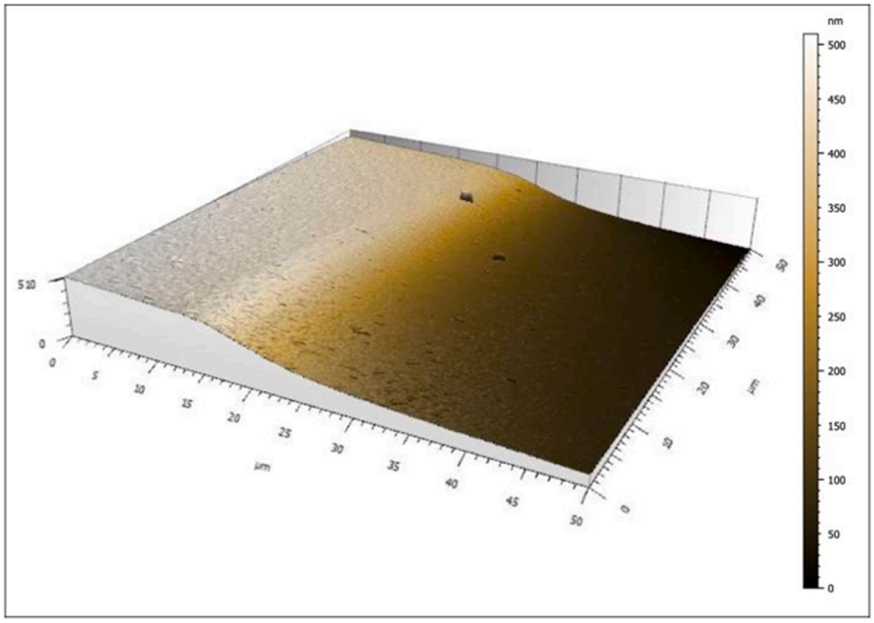

Fig. 7. Topography of the step between the silicon sample and the film in the AFM.

Table 2
Thickness values for layers deposited using HiPIMS and DC sources.

Source	HiPIMS	DC
Area 1	416.0 nm	152.9 nm
Area 2	443.0 nm	209.3 nm
Average value	**429.5 nm**	**181.1 nm**
Standard deviation	**19.1 nm**	**39.9 nm**

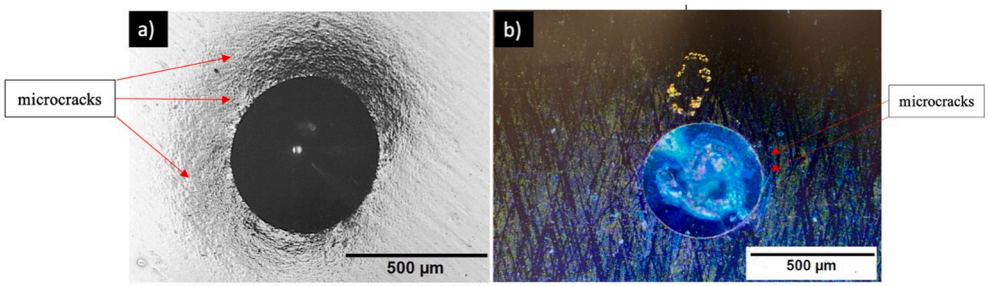

Fig. 8. Image of qualitative adhesion test of the deposited layer using (a) the HiPIMS source and (b) the DC source through the indentation on the Rockwell C durometer.

Table 3
Parameters used in scratch tests.

Source	Distance	Speed	Load
HiPIMS	5 mm	0.10 mm/s	0–50 N
DC	2 mm	0.33 mm/s	0–5 N

Table 4
Critical load values obtained in scratch tests.

Source	LC1	LC2
HiPIMS	1 N	35 N
DC	1 N	2 N

adequate speed and tools for a finishing with low roughness.

3.5. Fatigue tests

Fatigue tests were performed for three different conditions: without coating, with coating using the DC source and with coating using the HiPIMS source. Ten specimens were tested without coating, five with coating using the HiPIMS source, and six specimens with coating using the DC source. The results of the fatigue tests are presented in Table 5.

The uncoated specimens were tested initiating in a stress level around 89% the ultimate tensile strength, and in the range of 843.80–852.84 MPa. The stress range used for both coated conditions was from 798.60 MPa to 852.84 MPa. After carrying out the fatigue tests in the specimens with and without coating, the results of maximum stress per number of cycles until failure were placed as points on the S-N graph, shown in Fig. 9. The arrows indicate that the specimen did not fracture up to 10^6 cycles (run-out).

The Ti-6Al-4V alloy presents a well-defined fatigue limit. The study of the coated alloy was concentrated on stresses around this limit previously obtained on the uncoated alloy. Ti-6Al-4V alloy has fatigue endurance limit values, according to literature, which may vary according to the finishing, manufacture and surface treatments, ranging from 610 MPa to 950 MPa [5]. The fatigue endurance limit was high in all cases, taking the ultimate tensile strength tested (995 MPa) as a reference. The uncoated specimens had a fatigue endurance limit value of 843.80 MPa. The coated specimens using both sources (HiPIMS and DC) showed a decrease in the fatigue endurance limit, with a value of 798.60 MPa. It is not possible to state that this decrease is due to the coating, because of the small difference between the stresses.

Coating with ceramic thin films can cause a decrease in fatigue endurance limit in tests, but increase the number of cycles until fracture due to the brittle behavior of the coated material [28]. Considering Hooke's law:

$$\sigma = \mathrm{E} \cdot \varepsilon \tag{1}$$

where σ is the applied stress, E is the Young's modulus, and ε is the corresponding strain, it is possible to analyze the effect of stresses. As the Young's modulus of the ceramic layers is high, at higher stresses the crack propagation through the persistent slip bands causes the film to rupture, propagating the crack until the part fails. At lower stress levels, the film can stop such propagation, since the deformation caused is smaller, and the ceramic layer is not stressed to the point of rupture. Fig. 10 illustrates these mechanisms:

Farokhzadeh and Edrisy [29] nitrided the Ti-6Al-4V alloy at two different temperatures, and a substantial decrease in fatigue endurance limit of the nitrided specimens was observed due to premature failure of the nitrided surface layers compared to those without nitriding.

Castro et al. [6] observed that the nitrided specimens in the low-cycle fatigue region had a higher cycle number to failure than the non-nitrided specimens. However, for the fatigue endurance limit, the nitrided specimens showed lower values than the non-nitrided specimens. This same behavior was observed by Zuo et al. [30]. A possible explanation for this behavior may be related to the resistance of the nitrided layer, which when subjected to high stresses breaks, not delaying the crack initiation.

This behavior was notice by Yonekura et al. [11] and Zhou et al. [9], that studied the impact of multilayer films, of CrN/Cr and TiN/Ti respectively. The results show that the multilayered coating can increase the fatigue endurance limit of the materials significantly, while the bilayer coating has no obvious effect. The possible reason for this change, is that multilayer coats have more thickness made of ductile materials from the interlayers – Cr and Ti – which helps the film to have a higher deformation without breaking.

This can be noticed in the study of Lee et al. [14] that compares a metallic glass and TiN/Ti thin films with 200 nm of thickness. The

Table 5
Results of fatigue tests of Ti-6Al-4V alloy specimens uncoated and coated using HiPIMS and DC sources.

Stress (MPa)	Force (N)	Cycles without coating	Cycles with DC coating	Cycles with HiPIMS coating
798.60	26,500	–	1,000,000	1,000,000
813.67	27,500	–	544,877	313,448
843.80	28,000	1,000,000	744,937	326,324
846.82	28,100	256,527	568,741	67,053
849.83	28,200	180,017	578,738	113,921
852.84	28,300	83,975	627,330	–
858.87	28,500	73,488	–	–
873.94	29,000	36,692	–	–
889.01	29,500	60,000	–	–
904.08	30,000	37,500	–	–
919.14	30,500	23,774	–	–
934.21	31,000	19,733	–	–

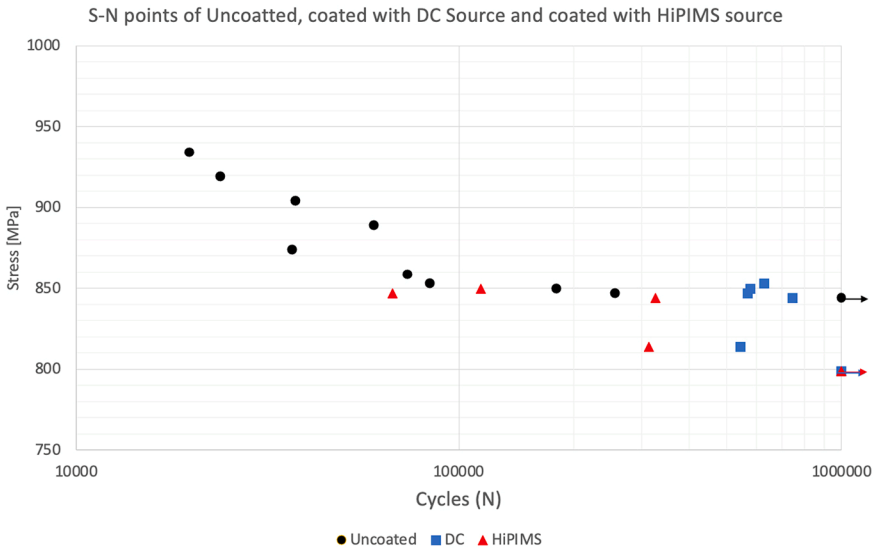

Fig. 9. Maximum stress graph in fatigue tests as a function of the number of cycles to failure. Arrows indicate that the test was stopped with 10^6 cycles without breaking (run-out specimen).

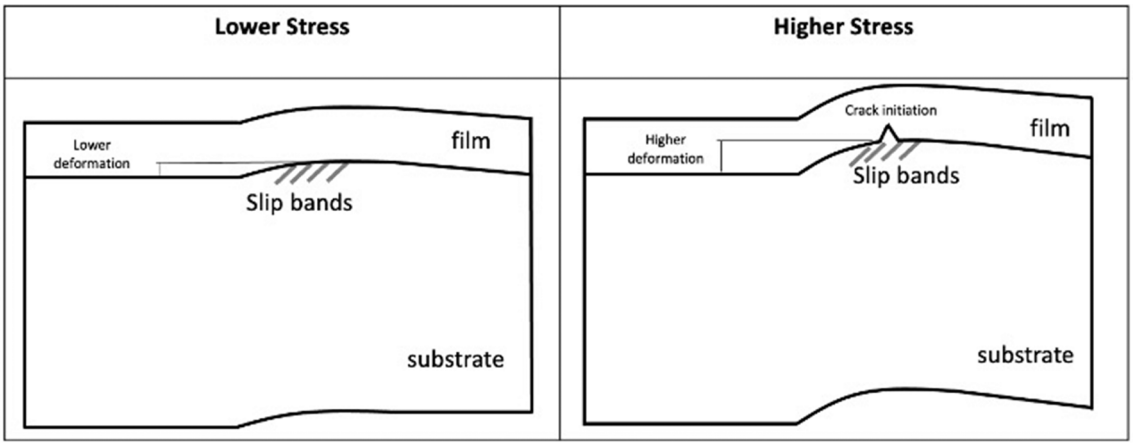

Fig. 10. Stress mechanism diagram.

metallic glass cover increased the number of cycles and the fatigue endurance limit, because of the ductility of the film. The ceramic film behaves as the other studies.

The observations of the fracture surfaces of SiC coated and uncoated specimens tested in fatigue, it will be possible to analyze the micromechanisms involved in the nucleation and propagation of cracks.

3.6. Fractographic analysis

Figs. 12–19 show the fracture surfaces of Ti-6Al-4V alloy specimens tested in fatigue under the 3 conditions investigated: uncoated, coated with SiC and Cr interlayer using the DC source and using the HiPIMS source. Fig. 11 shows the fracture surface of uncoated Ti-6Al-4V alloy specimens tested under fatigue with a maximum stress of 846.82 MPa. The arrows from the optical microscope fractography of Fig. 11(a) and 11(b) indicate the crack initiation region. In the fractography seen in Fig. 11(c), the same crack initiation region observed by SEM is observed. In Fig. 11(d), also observed by SEM, marks of fast crack propagation can be seen. The uncoated specimens had the beginning of the crack in the maximum stress tests of 846.82 MPa on the surface of the specimens. Fatigue studies show that the crack forms preferentially on the free surface However, the subsurface crack formation could be inhibited by the tensile bending stress on the surface balanced with the compressive residual stress of the coating with a well-bonded interface. [29]. This is because the residual stress delays the begging of the crack because the tensile stresses that will nucleate the cracks need to "overcome" the existing compressive residual stress. In this study, it was not possible to measure the residual stress by X-ray diffraction because the film thickness is very thin. In fractographic analyzes of the uncoated Ti-6Al-4V alloy, such cracks initiated on the surface of the

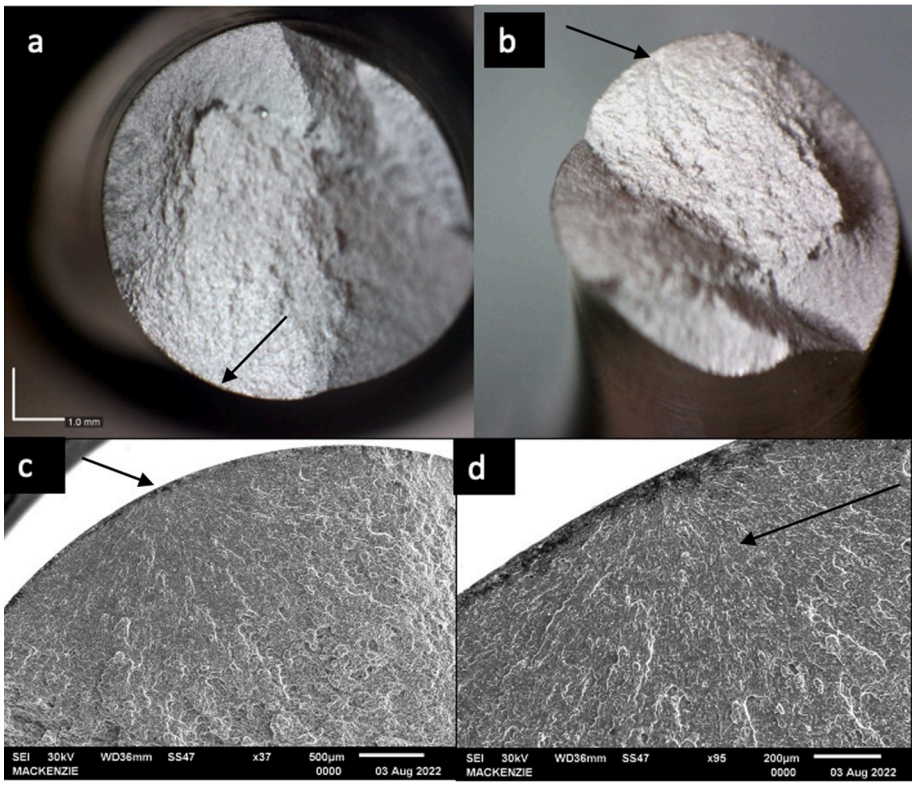

Fig. 11. Fracture surfaces of uncoated Ti-6Al-4V alloy specimen, fatigue tested with a maximum stress of 846.82 MPa. (a) and (b) Observations by OM, with arrows indicating the crack start location. (c) and (d) Observations by SEM, with the arrow indicating the beginning of the crack (c) and marks of fast crack propagation (d).

specimens were detected.

In the fatigue tests of Ti-6Al-4V alloy coated with SiC and Cr interlayer using the DC source, it was observed that the cracks originated in regions inside the specimens and not on their surface. The crack initiation and propagation region occur from an internal defect, for example an inclusion. The appearance of the fracture, also called "fish eye", can be observed in the images of Fig. 12 by optical microscopy and by scanning electron microscopy. In these images obtained by both MO and SEM, the arrows indicate the starting point of the crack, which propagates radially from this point. This type of fracture has been observed in nitrided specimens and in high cycle fatigue tests, where the specimen is tested for more than 10^8 cycles (100 million cycles). This behavior indicates a resistance to nucleation of cracks on the specimens surface due to the coating or due to low applied stresses, causing the crack to nucleate in a defect inside the specimen [31,32].

Tokaji and Takahashi [33] studied nitrided Cr-Mo steel with different nitriding times and, consequently, different layer thicknesses, tested under fatigue. In these studies, the presence of nucleated cracks in the internal regions of the specimens, with a "fish eye" aspect, was observed on the fracture surfaces of nitrided and fatigue tested specimens. This may occur because the TiN layer makes it difficult for the crack to nucleate on the surface.

In all specimens coated with SiC and Cr interlayer using the DC source and fractured in the fatigue tests, cracks began in non-surface regions due and the good adhesion of the film to the substrate after the test can be seen in Fig. 13.

Fig. 14 shows details of SiC film and Cr interlayer using the DC source on the fracture surface tested in fatigue with maximum stress of 852.54 MPa. In these images, the integrity and adhesion of the film to the substrate deposited using the DC source are evident. The adhesion to the substrate is decisive in the delay of crack nucleation in fatigue tests. In these images of the fractured specimens there is no evidence of delamination of the deposited layers. The fatigue results presented in Fig. 9 showed that the number of cycles of Ti-6Al-4V alloy specimens coated with SiC and Cr interlayer using the DC source was higher than the uncoated alloy specimens for the stress levels tested. All these data indicate a positive influence of the coating, which did not allow the surface nucleation of cracks by slip bands. The film did not break when the crack started, remaining adhered until the fracture and after the tests.

In the specimens of Ti-6Al-4V alloy coated with SiC and Cr interlayer using the HiPIMS source, it was possible to observe that the cracks, in general, originated on the surface, as observed in Fig. 15 (a) and (b). The only exception to crack initiation with the use of this coating occurred in the fatigue tests with a maximum stress of 813.67 MPa, as shown in Fig. 15 (c) and (d), it is observed that the crack nucleated inside the specimen, instead of starting on the surface. The SiC layer and Cr interlayer using the HiPIMS source proved to be less effective in delaying the nucleation of surface cracks than with the DC source, being suitable only at low maximum fatigue stresses (813.67 MPa). Castro et al. [6] in their study of nitrided Ti-6Al-4V alloy and tested in bending-rotating fatigue ($R = -1$) observed that

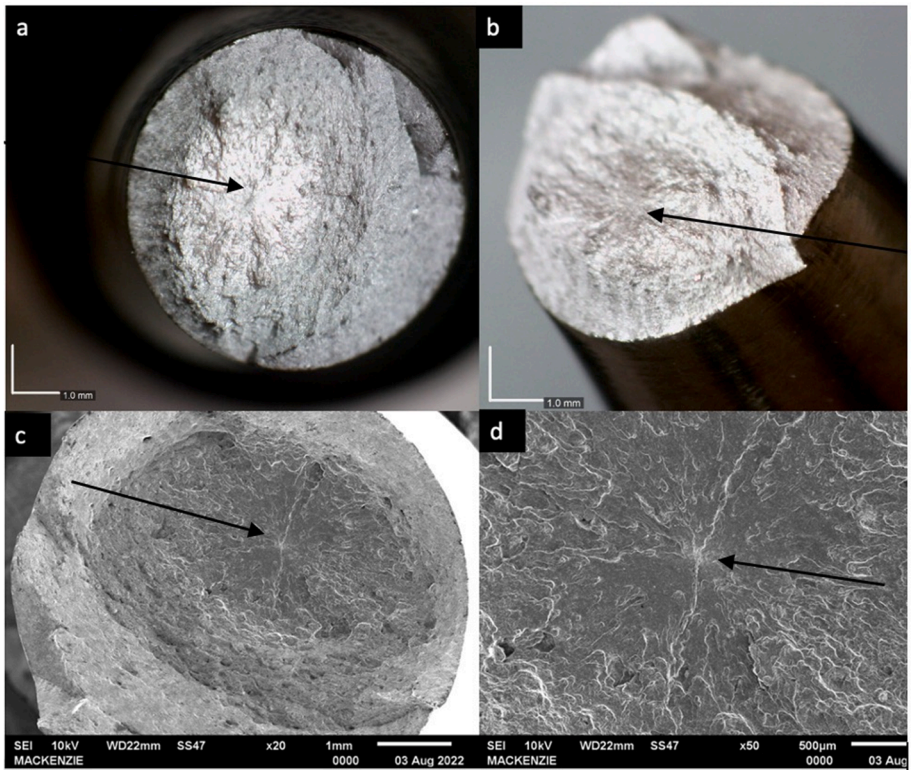

Fig. 12. Images of the fracture surfaces of the Ti-6Al-4V alloy specimens coated with SiC and Cr interlayer using the DC source and tested in fatigue with a maximum stress of 849.83 MPa, showing the region of crack initiation and propagation by OM (a and b) and by SEM (c and d).

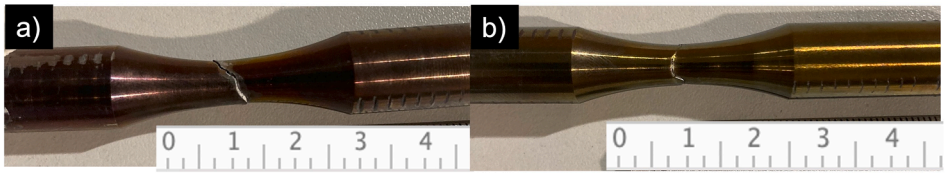

Fig. 13. Fatigue-tested specimens of Ti-6Al-4V alloy coated with SiC and Cr interlayer using the DC source, showing the adhesion of the film after fracture with a maximum stress of (a) 846.82 MPa and (b) 849.83 MPa.

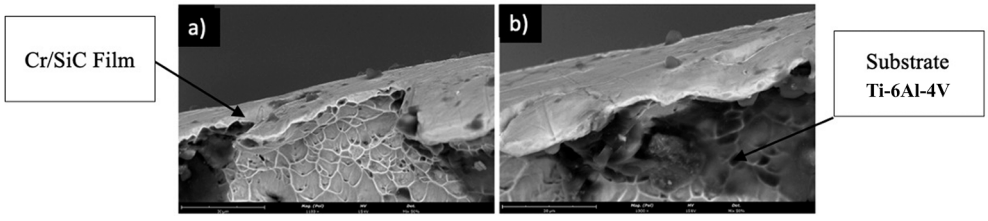

Fig. 14. Detail of the fracture surface of the Ti-6Al-4V alloy specimen coated with SiC and Cr interlayer using a DC source and fatigue tested with a maximum stress of 852.54 MPa, showing the film adhered to the substrate.

the fatigue cracking was initiated in a surface region, and the fracture surfaces showed an extensive region of flat propagation, followed by a relatively small region of final failure.

Fig. 16 shows images by SEM of the fracture surface of Ti-6Al-4V alloy specimens coated with SiC and Cr interlayer using HiPIMS source and tested under fatigue with maximum stresses of 846.82 MPa. The arrows indicate the beginning of the crack, which occurred on the surface, and it is also observed lines that indicate a fast propagation.

Fig. 17 (a) shows the fully delaminated thin film after the fatigue test with a maximum stress of 846.82 MPa. In the fatigue test with

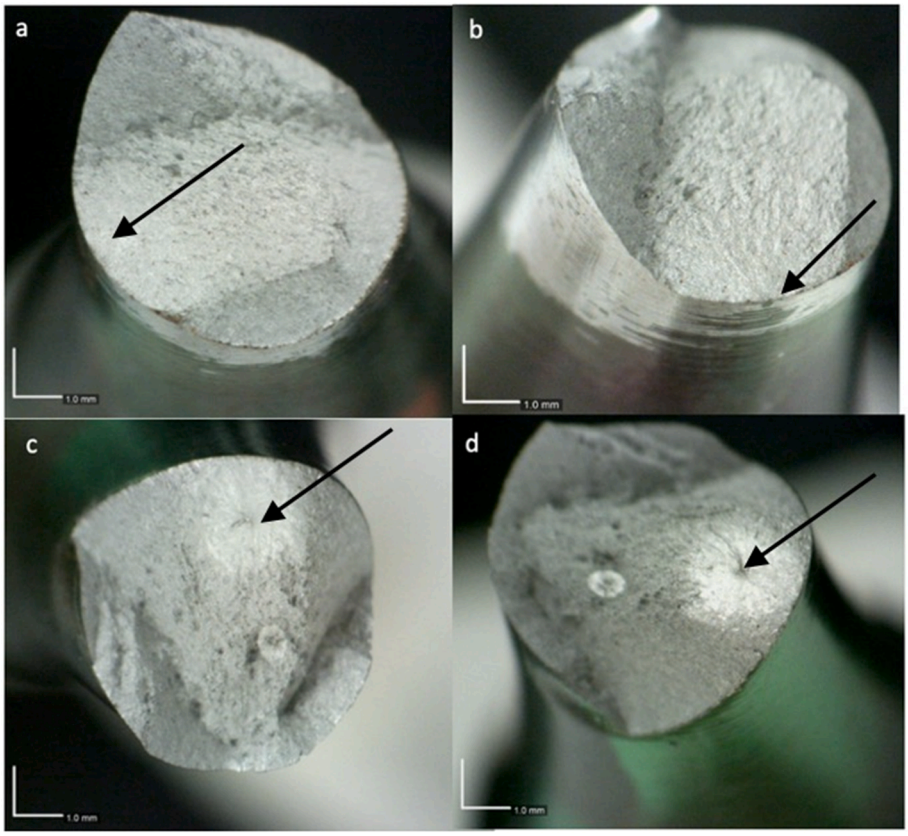

Fig. 15. Images observed by MO of the fracture surfaces of Ti-6Al-4V alloy specimens coated with SiC and Cr interlayer using HIPIMS source and tested in fatigue with maximum stresses of 846.82 MPa (a and b) and 813.67 MPa (c and d), with arrows indicating the crack initiation region.

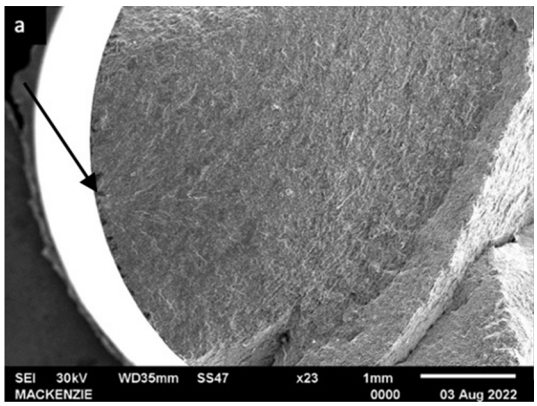

Fig. 16. Images observed by SEM of the fracture surfaces of Ti-6Al-4V alloy specimens coated with SiC and Cr interlayer using HIPIMS source and tested in fatigue with maximum stresses of 846.82 MPa.

maximum stress of 813.67 MPa, the thin film did not delaminate, remaining adhered even after the rupture, as can be seen in Fig. 17 (b). This indicates the importance of film adhesion, showing its influence on fatigue results.

Detailed images of the thin film observed in the SEM of the coating/substrate interface region of the specimen tested in fatigue (maximum stress of 813.67 MPa) of the Ti-6Al-4V alloy coated with SiC and Cr interlayer using a HiPIMS source is shown in Fig. 18. The film has no cracks at the interface between the surface of failure and the half of the ruptured part, demonstrating that its integrity was maintained, and it did not delaminate, positively influencing both the number of cycles to fracture and the crack initiation region. In the Ti-6Al-4V alloy specimens coated with SiC and Cr interlayer using the HiPIMS source, it appears that with higher stress application (846.82 MPa) the thin film fracture more quickly, and the crack started on the surface of the specimen. In the fatigue test

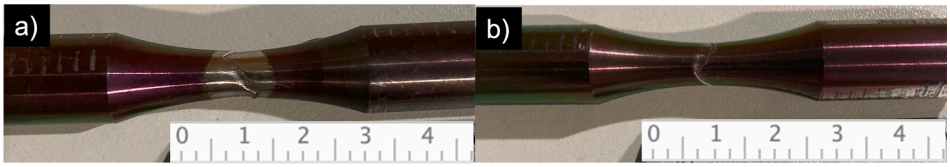

Fig. 17. Fatigue test specimens of Ti-6Al-4V alloy coated with SiC and Cr interlayer using the HIPIMS source, showing how the adhesion of the film is after fracture in fatigue tests with maximum stress of (a) 846.82 MPa and (b) 813.67 MPa.

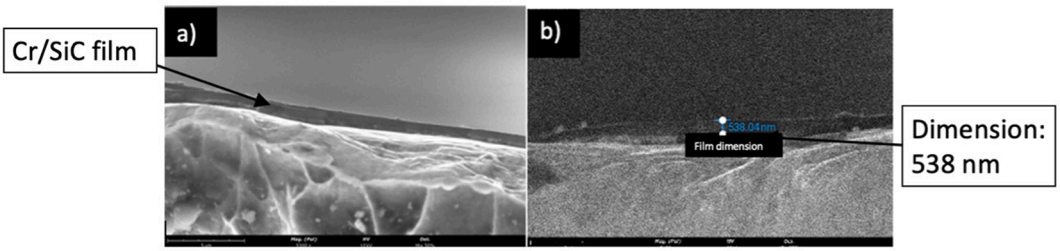

Fig. 18. Detailed images observed in the SEM of the coating/substrate interface region of the specimen tested in fatigue (maximum stress of 813.67 MPa) of Ti-6Al-4V alloy coated with SiC and Cr interlayer using HiPIMS source.

HiPIMS

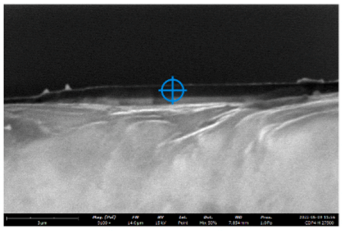

Element Symbol	Element Number	Atomic Concentration	Weight Concentration
C	Carbon	62.761	36.200
Si	Silicon	26.167	35.300
Ti	Titanium	2.608	6.000
Cr	Chrome	7.448	18.600
Br	Bromine	1.016	3.900

DC

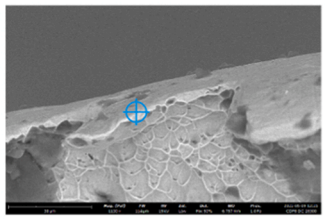

Element Symbol	Element Name	Atomic Concentration	Weight Concentration
C	Carbon	22.464	12.500
O	Oxygen	51.260	38.000
Al	Aluminum	0.800	1.000
Si	Silicon	8.759	11.400
Ti	Titanium	16.717	37.100

Fig. 19. EDS analysis of the film/substrate region of a fatigue test specimen of Ti-6Al-4V alloy coated with SiC and Cr interlayer using (a) HiPIMS source and (b) DC source.

with lower maximum stress (813.67 MPa), the thin film probably supported the stress, not breaking immediately, implying the beginning of the crack generated by internal defects in the specimen. Therefore, when the SiC and Cr interlayer films remain adhered during fatigue tests with applications of relatively low maximum stresses or when the layer is better adhered to the Ti-6Al-4V alloy, fractures start internally in the specimens, in the "fish-eye" shape and not on the surface.

3.7. Energy dispersive spectroscopy (EDS)

The X-ray diffractometry could not identify the present phases of the film because they are very thin and probably amorphous, so the EDS was included to have at least information about the chemical elements present in the film. Under the conditions in which it was possible to identify the film by SEM, EDS analyzes were performed to verify the elements present in the film and substrate region. Fig. 19 shows the graphs and tables resulting from the EDS analysis of the fatigue tested specimens of Ti-6Al-4V alloy coated with SiC and Cr interlayer using HiPIMS and DC sources, respectively. Through these graphs and tables of the elements present, it is possible to verify the existence of the elements that constitute the film, as well as to have an estimate of its chemical composition. In both analyzes there is an approximate relative stoichiometry of 1:1 between Carbon and Silicon, suggesting the existence of the SiC compound. It is also possible to notice the existence of Chromium, which composes the interlayer and Titanium of the substrate.

4. Conclusions

In the analysis of cracking failure due to fatigue of the Ti-6Al-4V alloy with SiC coating and Cr interlayer deposited by magnetron sputtering using two sources: DC and HiPIMS, the following conclusions can be drawn:

- SiC films with Cr interlayer deposited using HiPIMS and DC sources proved to be homogeneous. The average thickness of the SiC films with Cr interlayer was 429 nm using the HiPIMS source and 181 nm using the DC source.
- The number of cycles decreased in Ti-6Al-4V alloy specimens coated with SiC and Cr interlayer using the HIPIMS source in all investigated stress cycles.
- The film obtained using the DC source increased the number of cycles to fracture at the investigated stresses, when compared to the uncoated specimens.
- Cracks in the specimens covered with the use of DC source tested in fatigue started inside and not on the surface, with the characteristic of "fish-eye" shape. This indicates that the film prevented the cracks from starting on the surface, showing its efficiency compared to the uncoated alloy.
- In the specimens coated using the HiPIMS source, the cracks started mostly on the surface, with delamination of the SiC film and Cr interlayer and worsening the fatigue performance.
- Fish-eye fracture shape also occurred in fatigue tests with relatively low maximum stresses both in coated specimens using DC source and HiPIMS.

Declaration of Competing Interest

The authors declare that they have no known competing financial interests or personal relationships that could have appeared to influence the work reported in this paper.

Data availability

No data was used for the research described in the article.

Acknowledgments

This work was supported by:

- Coordination of Superior Level Staff Improvement (CAPES), Brazil - Finance Code 001 [grant number 88887.583658/2020-00].
- FCT, through IDMEC, under LAETA, project UIDB/50022/2020.

Appendix A. Supplementary material

Supplementary data to this article can be found online at https://doi.org/10.1016/j.engfailanal.2023.107325.

References

[1] H. Warlimont, Titanium and Titanium Alloys, Springer Handbooks, 2018, pp. 195–206. <https://doi.org/10.1007/978-3-319-69743-7_7>.
[2] V.M.C.A. De Oliveira, M.C.L. Da Silva, C.G. Pinto, P.A. Suzuki, J.P.B. Machado, V.M. Chad, M.J.R. Barboza, Short-term creep properties of Ti-6Al-4V alloy subjected to surface plasma carburizing process, J. Mater. Res. Technol. 4 (2015) 359–366, https://doi.org/10.1016/j.jmrt.2015.05.006.
[3] A. Sedmak, F. Vucetic, K. Colic, A. Grbovic, S. Sedmak, S. Kirin, F. Berto, Fatigue life assessment of orthopedic plates made of Ti6Al4V, Eng. Fail. Anal. 137 (2022), 106259, https://doi.org/10.1016/j.engfailanal.2022.106259.
[4] K. Praveenkumar, P. Mylavarapu, A. Sarkar, E. Isaac Samuel, A. Nagesha, S. Swaroop, Residual stress distribution and elevated temperature fatigue behaviour of laser peened Ti-6Al-4V with a curved surface, Int. J. Fatigue. 156 (2022), 106641, https://doi.org/10.1016/j.ijfatigue.2021.106641.
[5] P. Wieciński, J. Smolik, H. Garbacz, K.J. Kurzydłowski, Failure and deformation mechanisms during indentation in nanostructured Cr/CrN multilayer coatings, Surf. Coat. Technol. 240 (2014) 23–31, https://doi.org/10.1016/j.surfcoat.2013.12.006.
[6] M. de Castro, A. Couto, G. Almeida, M. Massi, N. de Lima, A. da Silva Sobrinho, M. Castagnet, G. Xavier, R. Oliveira, The effect of plasma nitriding on the fatigue behavior of the Ti-6Al-4V Alloy, Materials (Basel) 12 (2019) 520, https://doi.org/10.3390/ma12030520.
[7] V. Anes, L. Reis, B. Li, M. Freitas, Crack path evaluation on HC and BCC microstructures under multiaxial cyclic loading, Int. J. Fatigue. 58 (2014) 102–113, https://doi.org/10.1016/j.ijfatigue.2013.03.014.
[8] M.Y.P. Costa, M.L.R. Venditti, H.J.C. Voorwald, M.O.H. Cioffi, T.G. Cruz, Effect of WC–10%Co–4%Cr coating on the Ti–6Al–4V alloy fatigue strength, Mater. Sci. Eng. A. 507 (2009) 29–36, https://doi.org/10.1016/j.msea.2008.11.068.
[9] Y. Zhou, G.B. Rao, J.Q. Wang, B. Zhang, Z.M. Yu, W. Ke, E.H. Han, Influence of Ti/TiN bilayered and multilayered films on the axial fatigue performance of Ti46Al8Nb alloy, Thin Solid Films. 519 (2011) 2207–2212, https://doi.org/10.1016/j.tsf.2010.10.025.
[10] D. Zhu, B.A. Lerch, S. Kalluri, Fatigue Behavior of Coated Titanium Alloys, 2019, 18.
[11] D. Yonekura, J. Fujita, K. Miki, Fatigue and wear properties of Ti-6Al-4V alloy with Cr/CrN multilayer coating, Surf. Coat. Technol. 275 (2015) 232–238, https://doi.org/10.1016/j.surfcoat.2015.05.014.

[12] R.H. Oskouei, R.N. Ibrahim, Restoring the tensile properties of PVD-TiN coated Al 7075–T6 using a post heat treatment, Surf. Coat. Technol. 205 (2011) 3967–3973, https://doi.org/10.1016/j.surfcoat.2011.02.041.
[13] B.S. Saini, V.K. Gupta, Effect of WC/C PVD coating on fatigue behaviour of case carburized SAE8620 steel, Surf. Coat. Technol. 205 (2010) 511–518, https://doi.org/10.1016/j.surfcoat.2010.07.022.
[14] C.M. Lee, J.P. Chu, W.Z. Chang, J.W. Lee, J.S.C. Jang, P.K. Liaw, Fatigue property improvements of Ti-6Al-4V by thin film coatings of metallic glass and TiN: A comparison study, Thin Solid Films. 561 (2014) 33–37, https://doi.org/10.1016/j.tsf.2013.08.027.
[15] T. Sugahara, G.V. Martins, F.E. Montoro, A. Merij Neto, M. Massi, A.S. Silva Sobrinho, D.A.P. Reis, Creep behavior evaluation and characterization of SiC film with Cr interlayer deposited by HiPIMS in Ti-6Al-4V alloy, Surf. Coat. Technol. 309 (2017) 410–416, https://doi.org/10.1016/j.surfcoat.2016.11.091.
[16] C. Ma, C. Zhao, X. Fan, Z. Liu, J. Liu, Preparation of non-stoichiometric Al2O3 film with broadband antireflective by magnetron sputtering, Chem. Phys. Lett. 764 (2021), 138299, https://doi.org/10.1016/j.cplett.2020.138299.
[17] Y. Cao, Y. Xia, B. Duan, W. Mu, X. Tan, H. Wu, Microstructure evolution and anti-wear mechanism of Cu film fabricated by magnetron sputtering deposition, Mater. Lett. 315 (2022), 131941, https://doi.org/10.1016/j.matlet.2022.131941.
[18] A.C. Merij, T. Sugahara, G.V. Martins, A.S. da Silva Sobrinho, D.A.P. Reis, P.A.R. Gonçalves, M. Massi, Use of Cr interlayer to promote the adhesion of SiC films deposited on Ti-6Al-4V by HiPIMS, Mater. Res. 18 (2015) 904–907, https://doi.org/10.1590/1516-1439.313114.
[19] Y.Y. Wang, K. Kusumoto, C.J. Li, XPS analysis of SiC films prepared by radio frequency plasma sputtering, Phys. Proc. 32 (2012) 95–102, https://doi.org/10.1016/j.phpro.2012.03.524.
[20] VDI - Fachbereich Produktionstechnik und Fertigungsverfahren, VDI 3198 Coating (CVD, PVD) of Cold Forging Tools, 1992, 8.
[21] N. Vidakis, A. Antoniadis, N. Bilalis, The VDI 3198 indentation test evaluation of a reliable qualitative control for layered compounds, J. Mater. Process. Technol. 143–144 (2003) 481–485, https://doi.org/10.1016/S0924-0136(03)00300-5.
[22] K. Holmberg, A. Laukkanen, H. Ronkainen, K. Wallin, S. Varjus, J. Koskinen, Tribological contact analysis of a rigid ball sliding on a hard coated surface. Part I: Modelling stresses and strains, Surf. Coat. Technol. 200 (2006) 3793–3809, https://doi.org/10.1016/j.surfcoat.2005.03.040.
[23] H. Shibata, K. Tokaji, T. Ogawa, C. Hori, The effect of gas nitriding on fatigue behaviour in titanium alloys, Int. J. Fatigue. 16 (1994) 370–376, https://doi.org/10.1016/0142-1123(94)90448-0.
[24] H. Nan, C. Yuanru, C. Guangjun, L. Chenggang, W. Zhongguang, Y. Guo, S. Huehe, L. Xianghuai, Z. Zhihong, Research on the fatigue behavior of titanium based biomaterial coated with titanium nitride film by ion beam enhanced deposition, Surf. Coat. Technol. 88 (1997) 127–131, https://doi.org/10.1016/S0257-8972(96)02891-5.
[25] S. Peraud, P. Villechaise, J. Mendez, J. Delafond, Influence of thin coatings deposited by a dynamic ion mixing technique on the fatigue life of titanium alloys, J. Mater. Sci. 34 (1999) 1003–1008, https://doi.org/10.1023/A:1004535709821.
[26] J. Bohlmark, M. Lattemann, J.T. Gudmundsson, A.P. Ehiasarian, Y. Aranda Gonzalvo, N. Brenning, U. Helmersson, The ion energy distributions and ion flux composition from a high power impulse magnetron sputtering discharge, Thin Solid Films. 515 (2006) 1522–1526, https://doi.org/10.1016/j.tsf.2006.04.051.
[27] K.D. Bakoglidis, S. Schmidt, G. Greczynski, L. Hultman, Improved adhesion of carbon nitride coatings on steel substrates using metal HiPIMS pretreatments, Surf. Coat. Technol. 302 (2016) 454–462, https://doi.org/10.1016/j.surfcoat.2016.06.048.
[28] M. Rahman, I. Reid, P. Duggan, D.P. Dowling, G. Hughes, M.S.J. Hashmi, Structural and tribological properties of the plasma nitrided Ti-alloy biomaterials: Influence of the treatment temperature, Surf. Coat. Technol. 201 (2007) 4865–4872, https://doi.org/10.1016/j.surfcoat.2006.07.178.
[29] K. Farokhzadeh, A. Edrisy, Fatigue improvement in low temperature plasma nitrided Ti-6Al-4V alloy, Mater. Sci. Eng. A. 620 (2015) 435–444, https://doi.org/10.1016/j.msea.2014.10.008.
[30] J.H. Zuo, Z.G. Wang, E.H. Han, Effect of microstructure on ultra-high cycle fatigue behavior of Ti-6Al-4V, Mater. Sci. Eng. A. 473 (2008) 147–152, https://doi.org/10.1016/j.msea.2007.04.062.
[31] Z. Sun, W. Li, H. Deng, Z. Zhang, Fisheye failure analysis and life design approach for case-carburized gear steel based on statistical evaluation of defect size, Eng. Fail. Anal. 59 (2016) 28–40, https://doi.org/10.1016/j.engfailanal.2015.11.017.
[32] M. Avateffazeli, M. Haghshenas, Ultrasonic fatigue of laser beam powder bed fused metals: a state-of-the-art review, Eng. Fail. Anal. 134 (2022), 106015, https://doi.org/10.1016/J.ENGFAILANAL.2021.106015.
[33] K. Tokaji, S. Takahashi, Fatigue fracture process with fish-eye in gas-nitrided low alloy steel, Comput. Exp. Methods (2001) 171–180.